RSC Advances

PAPER

View Article Online
View Journal | View Issue

Cite this: *RSC Adv.*, 2017, **7**, 28696

A Ni-containing decaniobate incorporating organic ligands: synthesis, structure, and catalysis for allylic alcohol epoxidation†

Li Li, Yanjun Niu, Kaili Dong, Pengtao Ma, Chao Zhang, Jingyang Niu* and Jingping Wang*

Received 20th March 2017
Accepted 17th May 2017

DOI: 10.1039/c7ra03254d

rsc.li/rsc-advances

An organic–inorganic hybrid polyoxoniobate, $Na_8\{Ni[Ni(en)]_2Nb_{10}O_{32}\}\cdot 28H_2O$ (**1**) (en = ethanediamine), has been synthesized and characterized. It represents the first example of a trinuclear nickel-containing polyoxoniobate. The catalysis of **1** for allylic alcohol epoxidation was investigated at room temperature in aqueous solution, and was found to catalyze the epoxidation of 3-methyl-2-buten-1-ol with high conversion (98%) and selectivity (94%). Furthermore, magnetic measurements showed that the compound exhibits ferromagnetic interactions.

Introduction

Polyoxoniobates (PONbs), an important subclass of polyoxometalates (POMs), have been investigated since the last century due to their unique characteristics of high basicity and high surface charge endowing them with spectroscopic, magnetic, and catalytic properties.[1,2] Nevertheless, in comparison with other POMs, the development of PONbs is still in its infancy owing to difficulties in controlling their synthesis, especially the narrow working pH range of PONbs.[3] Generally, most of the reported PONbs focus on heteropolyoxoniobates with the typical examples $[XNb_{12}O_{40}]^{16-}$ (X = Si, Ge),[4a] $[Ti_2O_2][XNb_{12}O_{40}]^{12-}$ (X = Si, Ge),[4b,c] $[Nb_2O_2][SiNb_{12}O_{40}]^{10-}$,[4d] and $[SiNb_{18}O_{54}]^{14-}$.[4e] Up to now, isopolyoxoniobates including $[Nb_{10}O_{28}]^{6-}$,[5a] $[Nb_{20}O_{54}]^{8-}$,[5b] $[Nb_{24}O_{72}H_9]^{15-}$,[5c] $[HNb_{27}O_{76}]^{16-}$, $[H_{10}Nb_{31}O_{93}(CO_3)]^{23-}$,[5d] and $[Nb_{32}O_{96}H_{28}]^{4-}$ (ref. 2*b*) have been isolated. In addition, a number of transition-metal (TM)-containing PONbs have also been obtained. The few examples of the PONbs are $\{Ti_2Nb_8\}$,[6a] $\{TiNb_9\}$,[6b] $\{Ti_{12}Nb_6\}$,[6c] $\{V_3Nb_{12}\}$,[7a] $\{V_4Nb_6\}$,[7b] $\{V_4Nb_{10}\}$,[7c] $\{PV_2Nb_{12}\}$,[7d] $\{XV_8Nb_8\}$ (X = P, V),[7e] $\{PV_6Nb_{12}\}$,[7f] $\{VNb_{14}\}$,[7g] $\{V_8Nb_{48}\}$,[7h] $\{Cu_{24}Nb_{56}\}$, $\{Cu_{25.5}Nb_{56}\}$,[8a] $\{CuNb_{11}\}$,[8b] $\{Co_{14}Nb_{36}\}$,[9a] $\{Co_8Nb_{24}\}$,[9b] $\{NiNb_{12}\}$,[10a] $\{NiNb_9\}$,[10b] $\{Ni_{10}Nb_{32}\}$.[10c] Introducing TMs with d electrons into the reaction can enrich the diversity of structures and properties in polyoxoniobates.

On the other hand, POMs have been widely used as catalysts for epoxidation reactions with hydrogen peroxide in the past few years.[11a,b] Epoxide alcohols, as an important intermediate and final product of the organic chemical industry, have already been applied in the field of fine chemicals, such as components of cosmetic formulations for moister and cleaning of skin. Traditionally, one of the useful approaches for the synthesis of required epoxide alcohols is the epoxidation reactions of allylic alcohols in the presence of H_2O_2 as the oxidation agent.[11c–e] Therefore, we focus on the synthesis of TM-containing PONbs and expect to discover good efficiency in the catalytic epoxidation of allylic alcohols.

Herein, the sodium salt of nickel-decaniobate derivative $Na_8\{Ni[Ni(en)]_2Nb_{10}O_{32}\}\cdot 28H_2O$ (**1**) was obtained by the hydrothermal and diffusional method, which was composed of a $\{Ni[Ni(en)]_2\}$ cluster coordinated by two monolacunary $[Nb_5O_{18}]^{11-}$ units. Furthermore, the Ni^{2+} ions at both ends of the $\{Ni[Ni(en)]_2\}$ cluster are functionalized by one en molecule respectively, resulting in a pseudosandwich-type PONb-based organic–inorganic hybrid compound. Most notably, it represents the first example of trinuclear Ni-containing PONb and extends into a one-dimensional (1D) chain by high-nuclear sodium-clusters. Furthermore, the catalytic epoxidation of allylic alcohols has also been preliminary studied. To the best of our knowledge, this is the first example of the epoxidation of allylic alcohols using PONb as an efficient catalyst at room temperature in aqueous solution.

Results and discussion

Synthesis

An interesting TM-substituted PONb $Na_8\{Ni[Ni(en)]_2Nb_{10}O_{32}\}\cdot 28H_2O$ (**1**) was synthesized using the hydrothermal synthesis method by reaction of the SeO_2, $Ni(NO_3)_2\cdot 6H_2O$, and

Henan Key Laboratory of Polyoxometalate Chemistry, Institute of Molecular and Crystal Engineering, College of Chemistry and Chemical Engineering, Henan University, Kaifeng 475004, Henan, China. E-mail: jyniu@henu.edu.cn; jpwang@henu.edu.cn; Fax: +86-371-23886876

† Electronic supplementary information (ESI) available: Bond valence sum calculations of O and Ni (Tables S1 and S2), additional structural figures (Fig. S1 and S2), additional measurements (Fig. S3–S8, Tables S3 and S4), catalytic properties (Fig. S9, S10, Tables S5 and S6). CCDC 1526285 for **1**. For ESI and crystallographic data in CIF or other electronic format see DOI: 10.1039/c7ra03254d

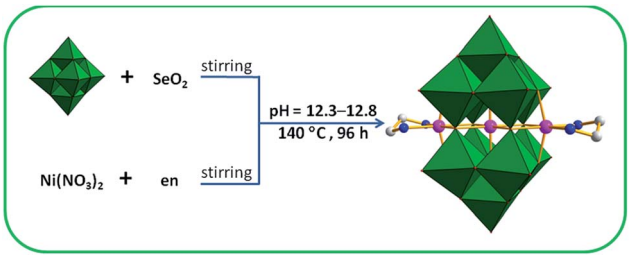

Scheme 1 The preparation process of **1**.

$K_7HNb_6O_{19}\cdot 13H_2O$ with the presence of en at the pH value of 12.3–12.8 (Scheme 1). Parallel experiments show that the final product depend on three key factors: (a) the introduction of en ligand. Its presence during the course of the reaction is crucial because the polyoxoanion could not be obtained if 1,2-diaminopropane or 1,3-diaminopropane was used to replace it or in the absence of it; (b) using NaOH solution to adjust pH value. Its presence is necessary to obtain pure bulk samples and the crystals could not be gained when NaOH solution was replaced by LiOH, KOH, or CsOH solution. The results confirm that counter cations can have significant effects on the synthesis; (c) the presence of SeO_2. Notably, although SeO_2 was used as a staring material in the system, no selenium atom was observed in the compound. When SeO_2 was removed from the reaction, no crystals were afforded. The specific role of SeO_2 was not well understood, and SeO_2 may play a synergistic action with other materials in the reaction and the similar phenomena have been previously reported.[12]

Crystal structure

Single-crystal X-ray diffraction analysis indicates that the structure of compound **1** possesses a cluster of $\{Ni[Ni(en)]_2Nb_{10}O_{32}\}$ along with eight Na^+ cations and twenty-eight water molecules. Compound **1** crystallizes in the triclinic molecular symmetry, $P\bar{1}$ space group. The $\{Ni[Ni(en)]_2Nb_{10}O_{32}\}$ cluster is constructed by a $\{Ni[Ni(en)]_2\}$ cluster sandwiched into the novel $\{Nb_{10}O_{32}\}$ fragment (Fig. 1a). And the $\{Nb_{10}O_{32}\}$ unit can be described as $\{W_{10}O_{32}\}$ reported by Fuchs *et al.*[13] It consists of two equivalent lacunary $[Nb_5O_{18}]^{11-}$ subunits fused together by four bridging oxygen atoms and the $[Nb_5O_{18}]^{11-}$ unit is obtained by removal of one $\{NbO_6\}$ octahedron from well-known Lindqvist anion $[Nb_6O_{19}]^{18-}$ (Fig. S1†). There are four types of oxygen atoms in the $\{Ni[Ni(en)]_2Nb_{10}O_{32}\}$ unit: ten terminal oxygen atoms (O_t), twelve bridging μ_2-oxygen atoms, four bridging μ_3-oxygen atoms, four bridging μ_4-oxygen atoms, and two central μ_6-oxygen atom. The bond lengths of Nb–O_t, Nb–μ_2-O, Nb–μ_3-O, Nb–μ_4-O and Nb–O_c in $\{Ni[Ni(en)]_2Nb_{10}O_{32}\}$ are in the range of 1.766(5)–1.773(5) Å, 2.029(4)–2.032(4) Å, 2.052(4)–2.098(4) Å, 1.929(4)–2.012(4) Å and 2.350(4)–2.410(4) Å. In the $\{Ni[Ni(en)]_2\}$ cluster, three nickel ions constitute a linear $\{Ni_3\}$ cluster *via* four bridging oxygen atoms (Fig. 1b). The Ni ions in $\{Ni[Ni(en)]_2\}$ cluster are all in the octahedral coordination environment, Ni1 ion is coordinated by four μ_2-O and two central oxygen atoms from two $[Nb_5O_{18}]^{11-}$ units (Fig. 1c) and Ni2 ions are completed by two N atoms from an en ligand and four O oxygen atoms from two $[Nb_5O_{18}]^{11-}$ skeletons (Fig. 1d).

As shown in Fig. 2, the adjacent cluster anions in **1** are linked alternately *via* $\{Na_8\}$ clusters into one-dimensional (1D) chain. It represents the first example of a high-nuclear sodium-cluster-containing in PONb. The Na^+ ions in the $\{Na_8\}$ cluster could be divided into four groups according to the difference between their coordinated environments. The Na1, Na2 and Na3 ions are all embedded in octahedral geometries with different coordination environments whereas Na4 ions exhibit a square pyramid geometry. On the one hand, Na1 and Na2 ions links each other by sharing two μ_2-O atoms forming a type of $[Na_2]^{2+}$ dimeric clusters in the edge-sharing mode, meanwhile the adjacent $[Na_2]^{2+}$ clusters are connected by two μ_2-O atoms generating a $[Na_4]^{4+}$ tetrameric cluster. On the other hand, Na3 and Na4 ions also join together by sharing two μ_2-O atoms forming another type of $[Na_2]^{2+}$ dimeric clusters. Moreover, one

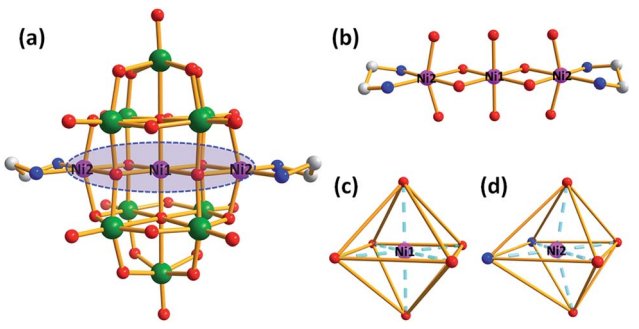

Fig. 1 (a) Ball-and-stick representation of the $\{Ni[Ni(en)]_2Nb_{10}O_{32}\}$ unit; (b) view of the $\{Ni[Ni(en)]_2\}$ cluster in **1**; (c) the coordinated environment of Ni1 in **1**; (d) the coordinated environment of Ni2 in **1**. All hydrogens, sodium ions, and lattice water molecules are omitted for clarity. Colour code: Nb (green), Ni (pink), N (blue), C (gray) and O (red).

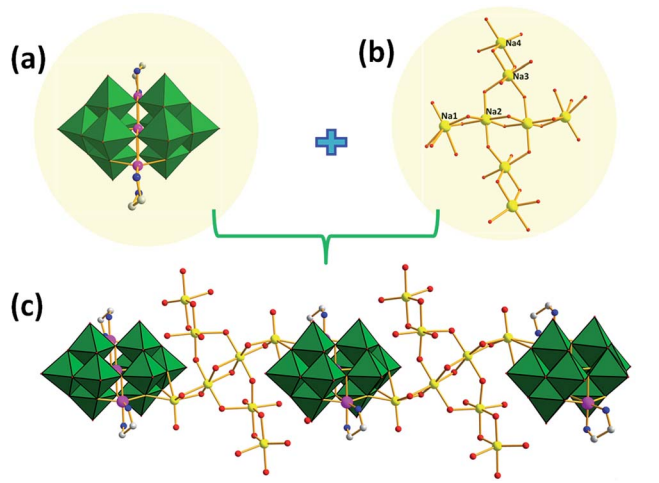

Fig. 2 (a) Combined polyhedral/ball-and-stick representation of the $\{Ni[Ni(en)]_2Nb_{10}O_{32}\}$ unit; (b) ball-and-stick representation of the $\{Na_8\}$ cluster; (c) combined polyhedral/ball-and-stick representation of one-dimensional (1D) of **1**. All hydrogens, and lattice water molecules are omitted for clarity. Colour code: Nb (green), Ni (pink), N (blue), C (gray), Na (yellow) and O (red) respectively.

$[Na_4]^{4+}$ and two $[Na_2]^{2+}$ dimeric clusters are connected by sharing four μ_2-O atoms forming the $\{Na_8\}$ cluster and displaying a unique cruciform structure.

The phase purity of **1** was characterized by the powder X-ray diffraction (PXRD) pattern of the bulk products (Fig. S3†). The PXRD pattern is in good agreement with the simulated XRPD patterns resulted from single-crystal X-ray diffraction, which confirms that the phase is pure. And the difference in intensity may be due to the preferred orientation of the powder samples. The band valence sum (BVS) calculations of compound **1** confirm that the oxidation states of the Ni and Nb atoms are +2, +5, respectively.[14] The BVS values for all oxygen atoms and nickel atoms in **1** are also listed in Tables S1 and S2.†

IR and UV spectra

The infrared spectrum of compound **1** was recorded between 4000 and 400 cm^{-1} with KBr pellet. The IR spectra shows seven characteristic vibration bands in the low-wavenumber region ($\nu < 1000$ cm^{-1}) belonging to the Lindqvist hexaniobate structure, the peak at 867 cm^{-1} can be assigned to terminal Nb–O_t characteristic vibration, as well as peaks at 667–419 cm^{-1} can be attributed to bridging Nb–O_b vibration. In comparison with the precursor $K_7HNb_6O_{19}\cdot 13H_2O$, the bridging Nb–$O_b$ vibration band splits into more components and shows slightly red shifts, which may originate from the coordination of Ni^{2+} with the bridging oxygen atoms of the PONb anion.[15] Moreover, the peaks at 1025 cm^{-1} can be assigned to C–N bond characteristic vibration of organic-ligand en (Fig. S4†).

UV-vis absorption spectrum of compound 1 (3×10^{-6} mol L^{-1}) in the aqueous solution displays one strong absorption band at 192 nm and one wide absorption band at 225 nm (Fig. S5 and S6†), which can be tentatively assigned to the pπ–dπ charge-transfer transitions of oxygen-to-niobium bonds.[12b] In comparison with UV spectra of the precursor $K_7HNb_6O_{19}\cdot 13H_2O$, the absorption band at 225 nm shows slightly blue shifts, which results from the coordination of Ni^{2+} with the oxygen atoms of the PONb anion.[15]

ESI-MS studies

During the course of this study, negative electrospray ionization mass spectrometry (ESI-MS) allowed us to identify intact polyanions $\{Ni[Ni(en)]_2Nb_{10}O_{32}\}$.[16] The compound **1** was dissolved in a minimum amount of water, and a few drops of this aqueous solution were mixed with acetonitrile ($V(H_2O) : V(CH_3CN) = 1 : 1$). ESI-MS data shows two dominant series of multiply charged peaks which can be attributed to series of peaks for −3 and −2 charged ions (Fig. 3). The series of −3 and −2 ion peaks can be attributed to $\{Na_xH_yNi[Ni(en)]_2Nb_{10}O_{32}\}^{3-}$ ($x + y + 3 = 8$), $\{Na_xH_yNi[Ni(en)]_2Nb_{10}O_{32}\}^{2-}$ ($x + y + 2 = 8$) polyanions on the basis of their m/z values, showing the presence of intact cluster in the mixture solution. Primary peaks centered at m/z 587.95 and 904.45 are clearly observed in the m/z 0–1500 range (Fig. 3, S7 and S8†). The extended peaks at around m/z 587.95 and 904.45 are provided in the ESI (Tables S3 and S4†).

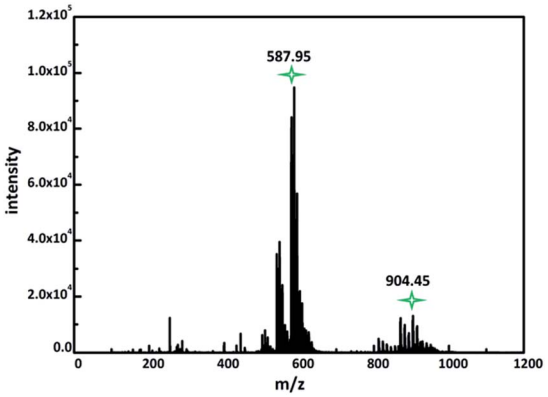

Fig. 3 The ESI mass spectrum of $\{Ni(Nien)_2Nb_{10}O_{32}\}$ in the range of $m/z = 0$–1500.

Magnetic properties

The magnetic susceptibility for **1** was measured at 2–300 K under a 1000 Oe magnetic field. Their plots of $\chi_M T$ and $\chi_M{}^{-1}$ *versus* T are illustrated in Fig. 4. Along with the temperature decreased, the $\chi_M T$ product of **1** increased from 5.355 emu K mol^{-1} at 300 K to a maximum of 8.622 emu K mol^{-1} at 5 K. This characteristic thermal behavior is indicative of an overall ferromagnetic coupling between nickel ions.[17] Upon the temperature lower than 5 K, the rapid drop of the $\chi_M T$ products may also be assigned to zero-field splitting. The experimental data have been well fitted by the Curie Weiss law ($\chi_M = C/(T - \theta)$) above 1.8 K with the following Curie and Weiss constants: 5.234 emu mol^{-1} K and 5.317 K, respectively (Fig. 4 and S9†). The positive Weiss constant confirms the presence of the ferromagnetic couplings between Ni^{2+} centers.[18] When the experimental $\chi_M T$ value of 5.355 emu K mol^{-1} at room temperature (300 K) is compared with that of the spin-only value of 3 emu K mol^{-1} for 3 non-interacting Ni^{2+} ions ($S = 1$) with $g = 2.0$, we can see that the experimental $\chi_M T$ value is higher than the calculate $\chi_M T$ value. So there exist spin–orbit coupling and ferromagnetic couplings among Ni^{2+} ions.[9b,10c]

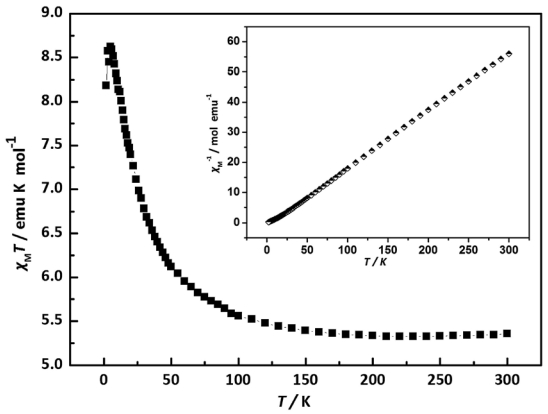

Fig. 4 The plots of $\chi_M T$ and $\chi_M{}^{-1}$ *versus* T for **1** between 2 and 300 K. (outside: $\chi_M T$; inside: $1/\chi_M{}^{-1}$).

Catalytic properties

Compound **1** was investigated as a heterogeneous catalyst in allylic alcohols epoxidation with H_2O_2 and allylic alcohols can be transform to epoxy alcohols as major products and the corresponding aldehydes and polyols were formed together as by-products (Table S5†). Initial experiments were carried out by using 3-methyl-2-buten-1-ol as a model substrate with the assistance of H_2O_2. Furthermore, the results of a series of parallel experiments showed that the conversion increased as the catalyst or H_2O_2 dosage increased (Table 1, entries 1–3 and 6), and didn't change obviously with the increase of reaction temperature and reaction time. As shown in Table 1, 3-methyl-2-buten-1-ol was oxidized to epoxy alcohol with 98% conversion and 94% selectivity at a temperature of 25 or 35 °C for 5 min (entries 3 and 7). This fact indicated that the conversion and selectivity of transformation to epoxide cannot achieve an obviously higher level as expected when the temperature is significantly higher than 25 °C. Moreover, the performance of epoxidation under low temperature ensures better security and allows the reduction of operating costs, so the temperature of 25 °C is the optimal reaction temperature. On the basis of these results, the catalyst and H_2O_2 dosage were the crucial factors for the conversion of epoxy alcohols. In contrast to catalyst **1**, a blank experiment without **1** (Table 1, entry 5) indicated that the epoxidation scarcely happened and the epoxidation reaction with the precursor $K_7HNb_6O_{19}\cdot 13H_2O$ indicated that the conversion was 95% (Table S6,† entry 3). As a result, the conversion of allylic alcohols epoxidation reactions of **1** was better than that of $K_7HNb_6O_{19}\cdot 13H_2O$, which suggests that Nb atoms play the main role in the process of the epoxidation reactions. Under optimal conditions (12 μmol catalyst, 5 mmol substrate and 8 mmol H_2O_2), 3-methyl-2-buten-1-ol was oxidized to epoxide with 98% conversion and 94% selectivity at 25 °C for 5 min (Table 1, entry 3). After the epoxidation reaction, the product was separated from the aqueous phase by extraction with ethyl acetate. And the catalyst still existed in the aqueous solution after extraction, so the aqueous phase could be used for the next run.[19] The catalytic activity of compound **1** was not obviously changed upon completion of the sixth run (Fig. S10†), but the catalytic activity of $K_7HNb_6O_{19}\cdot 13H_2O$ was decreased upon the process of duplicate operation (Fig. S11†). After epoxidation was completed, the catalyst was retrieved from the solvent/oxidant/substrate system by centrifugation. According to the comparisons of IR spectra of the fresh catalyst and the used catalyst after the sixth-run reaction (Fig. S12†), the noticeable differences of the IR spectrum are at the peaks of 1388 and 668 cm^{-1}. The results suggested that the framework structure of the catalyst was partially decomposed. The reason for the differences in IR spectra may be that the recovered catalyst has been partly peroxidated by H_2O_2.[20]

The catalytic activities of other allylic alcohols like 2-methyl-2-propen-1-ol, *trans*-2-hexen-1-ol and crotyl alcohol were also tested under the same reaction conditions (Tables 1 and S8†). The results showed that **1** was active for these allylic alcohols as well (Table 1, entries 8–10). 3-Methyl-2-buten-1-ol affords the highest epoxide yields and selectivity, while 2-methyl-2-propen-1-ol and *trans*-2-hexen-1-ol are less reactive corresponding to 36% conversion and 94% selectivity (Table 1, entry 8) and 41%

Table 1 Epoxidation of various allylic alcohols with H_2O_2 in water catalyzed by compound **1**

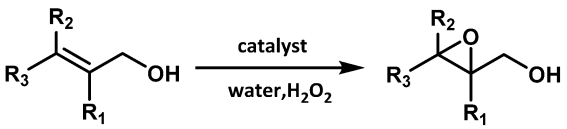

Entry	Substrate	Product	30%H_2O_2 (mmol)	Time (min)	Con.[a] (%)	Sel. (%)
1[b]			3	5	36	94
2			5	5	80	94
3			8	5	98	94
4	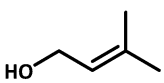	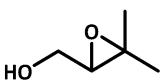	8	15	97	94
5[c]			8	5	5	60
6[d]			8	5	84	93
7[e]			8	5	98	94
8	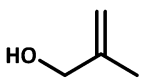	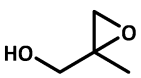	8	60	36	94
9	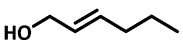	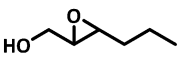	8	60	41	93
10[f]	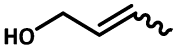	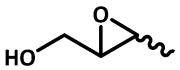	8	60	71	81

[a] Conversion determined by GC with dodecane as an internal standard. The products were identified by GC-MS. [b] Reaction conditions for the entries 1 to 5: catalyst (12 μmol), substrate (5 mmol) and H_2O (3 mL) at 25 °C. [c] Blank experiment, the reaction was carried out without catalyst. [d] Reaction conditions: catalyst (6 μmol), substrate (5 mmol) and H_2O (3 mL) at 25 °C. [e] Reaction conditions for the entries 7 to 10: catalyst (12 μmol), substrate (5 mmol) and H_2O (3 mL) at 35 °C. [f] *cis*- and *trans*-mixture.

conversion and 93% selectivity (Table 1, entry 9), respectively. In addition, crotyl alcohol gave 71% conversion and 81% selectivity (Table 1, entry 10). This result suggests that **1** can efficiently catalyze allylic alcohols epoxidation. Comparing with the reactivity for other allylic alcohols of catalyst **1** and $K_7HNb_6O_{19}\cdot 13H_2O$, the reactivity of $K_7HNb_6O_{19}\cdot 13H_2O$ is slightly higher than that of catalyst **1** (Table S8†). After epoxidation was completed, hydrogen peroxide consumption was determined iodometrically,[21] and the results indicated that the conversion of transformation to epoxy alcohols is related to the consumption of hydrogen peroxide (Table S9†).

Experimental section

Materials and methods

The raw material $K_7HNb_6O_{19}\cdot 13H_2O$ were prepared as described in the literature and characterized by IR spectrum.[22] All chemicals were purchased from commercial sources and used as received. Elemental analyses (C, H, N) were performed on an Elementar Vario EL cube CHNS analyzer. The IR spectrum was recorded on a Bruker-Vertex 70 FT-IR spectrometer using KBr pellets in a range of 4000–400 cm^{-1}. The UV spectra were recorded with a U1900 spectrometer (distilled water as solvent) in the range of 800–190 nm. Powder X-ray diffraction (PXRD) data were recorded on a Bruker AXS D8 Advance instrument with Cu Kα radiation ($\lambda = 1.5418$ Å) in the angular range $2\theta = 5$–50° at 293 K. Variable-temperature magnetic susceptibility data were obtained on Quantum Design MPMS3 magnetometer in the temperature range of 1.8–300 K with an applied field of 1000 Oe. The mass spectrometer used for the measurements was AB SCIEX Triple TOF 4600. The epoxidation products were identified by Agilent Technologies 7890B/5977B GC-MS instrument, and the conversion determined by BRUKER 450-GC instrument.

Synthesis of compound 1. $Ni(NO_3)_2\cdot 6H_2O$ (0.175 g) was added in distilled water (0.833 mL) under stirring. When the solid is dissolved, en (0.23 mL) was added to obtain the amaranthine solution. Then the resulting solution was added dropwise to the solution of $K_7HNb_6O_{19}\cdot 13H_2O$ (0.137 g, 0.1 mmol) and SeO_2 (0.045 g, 0.4 mmol) in water (10 mL) under stirring. Subsequently, the pH value of the mixture was adjusted to 12.3–12.8 using NaOH (2 mol L^{-1}) solution and then stirred for about 30 min. The mixture was put into a Teflon-lined autoclave (23 mL) and kept at 140 °C for 96 h, then cooled to room temperature and filtered. After that, the filtrate was transferred to a straight glass tube, ethanol/water (1 : 3) was carefully layered onto the resulting amaranthine solution, and then the pure alcohol was layered onto the ethanol/water phase. After about one month the light-blue crystals are found in the test tube. Yield: 54% (based on $K_7HNb_6O_{19}\cdot 13H_2O$). Elemental analysis (%) calculated for compound **1**: C 1.98, H 2.99, N 2.31; found for C 1.83, H 2.94, N 2.28. Selected IR (KBr, cm^{-1}): 3248 (*vs.*), 2174 (m), 1663 (s), 1585 (w), 1458 (w), 1023 (s), 867 (s), 775 (w), 667 (s), 621 (w), 546 (m), 483 (m), 419 (m).

X-ray crystallography

A suitable single crystal was selected from its mother liquor and sealed in a thin glass tube since the crystal is easily efflorescent. X-ray diffraction intensity data collection were mounted on a Bruker Apex-II CCD diffractometer using graphite-monochromatized Mo Kα radiation ($\lambda = 0.71073$ Å) at 293(2) K (Table 2). Routine Lorentz and polarization corrections were applied, and a multi-scan absorption correction was performed using the SADABS program. The structure was solved by direct methods and refined by the full-matrix least-squares method on F^2 using the SHELXS-97 and SHELXL-2014 program suite.[23] In the final refinement, the Nb and Na atoms were refined anisotropically; the O, C and N atoms were refined isotropically. The hydrogen atoms of the organic groups were placed in calculated positions and then refined using a riding model with a uniform value of $U_{iso} = 1.2$ or $1.5U_{eq}$. All H atoms on water molecules were directly included in the molecular formula.

Table 2 Crystal structure data for compound **1**

Formula	$C_4N_4Nb_{10}Ni_3O_{60}H_{72}Na_8$
M_r (g mol^{-1})	2425.80
T (K)	293(2)
Space group	$P\bar{1}$
Crystal system	Triclinic
a (Å)	12.5635(8)
b (Å)	12.9279(9)
c (Å)	13.1370(9)
α (deg)	61.8590(10)
β (deg)	63.6420(10)
γ (deg)	61.2230(10)
V (Å^3)	1582.83(19)
Z	1
D_c (g cm^{-3})	2.545
μ (mm^{-1})	2.783
F (000)	1186.0
2θ range (deg)	3.664 to 50.196
Data/restraints/parameters	5578/0/238
Reflections collected	8189
Index ranges	$-14 \le h \le 14$, $-15 \le k \le 15$, $-13 \le l \le 15$
GOF on F^2	1.021
R_1, wR_2 [$I > 2\sigma(I)$]	$R_1 = 0.0411$, $wR_2 = 0.0992$
R_1, wR_2 [all data]	$R_1 = 0.0545$, $wR_2 = 0.1077$

Conclusions

In summary, we have synthesized and characterized a novel organic–inorganic hybrid PONb which contains trinuclear nickel cluster. Furthermore, compound **1** shows catalytic activity for the epoxidation of various allylic alcohols with hydrogen peroxide. The successful synthesis of compound **1** enriches the structural diversity of PONbs and further proves that the use of metal–ligand cations could provide new way to synthesize diverse PONb anion architecture. In the following work, we will concentrate on improving the activity and selectivity for allylic alcohols epoxidation and the synthesis of novel PONb derivatives.

Acknowledgements

We gratefully acknowledge the National Natural Science Foundation of China (21371048), Key Lab of Polyoxometalate Science

of Ministry of Education, the Natural Science Foundation of Henan Province for financial support.

Notes and references

1 (*a*) C. A. Ohlin, E. M. Villa, J. C. Fettinger and W. H. Casey, *Angew. Chem., Int. Ed.*, 2008, **47**, 8251; (*b*) A. Flemming and M. Köckerling, *Angew. Chem., Int. Ed.*, 2009, **48**, 2605; (*c*) D.-Y. Du, J.-S. Qin, S.-L. Li, Z.-M. Su and Y.-Q. Lan, *Chem. Soc. Rev.*, 2014, **43**, 4615.

2 (*a*) L. Jin, X.-X. Li, Y.-J. Qi, P.-P. Niu and S.-T. Zheng, *Angew. Chem., Int. Ed.*, 2016, **55**, 13793; (*b*) P. Huang, C. Qin, Z.-M. Su, Y. Xing, X.-L. Wang, K.-Z. Shao, Y.-Q. Lan and E.-B. Wang, *J. Am. Chem. Soc.*, 2012, **134**, 14004; (*c*) J.-Q. Shen, Q. Wu, Y. Zhang, Z.-M. Zhang, Y.-G. Li, Y. Lu and E.-B. Wang, *Chem.–Eur. J.*, 2014, **20**, 2840; (*d*) D. Zhang, F. Cao, P. Ma, C. Zhang, Y. Song, Z. Liang, X. Hu, J. Wang and J. Niu, *Chem.–Eur. J.*, 2015, **21**, 17683.

3 M. Nyman, *Dalton Trans.*, 2011, **40**, 8049.

4 (*a*) M. Nyman, F. Bonhomme, T. M. Alam, J. B. Parise and G. M. B. Vaughan, *Angew. Chem., Int. Ed.*, 2004, **43**, 2787; (*b*) M. Nyman, F. Bonhomme, T. M. Alam, M. A. Rodriguez, B. R. Cherry, J. L. Krumhansl, T. M. Nenoff and A. M. Sattler, *Science*, 2002, **297**, 996; (*c*) W. Guo, H. Lv, K. P. Sullivan, W. O. Gordon, A. Balboa, G. W. Wagner, D. G. Musaev, J. Bacsa and C. L. Hill, *Angew. Chem., Int. Ed.*, 2016, **55**, 7403; (*d*) Z. Zhang, Q. Lin, D. Kurunthu, T. Wu, F. Zuo, S.-T. Zheng, C. J. Bardeen, X. Bu and P. Feng, *J. Am. Chem. Soc.*, 2011, **133**, 6934; (*e*) Y. Hou, M. Nyman and M. A. Rodriguez, *Angew. Chem., Int. Ed.*, 2011, **50**, 12514.

5 (*a*) E. J. Graeber and B. Morosin, *Acta Crystallogr., Sect. B: Struct. Crystallogr. Cryst. Chem.*, 1977, **33**, 2137; (*b*) M. Maekawa, Y. Ozawa and A. Yagasaki, *Inorg. Chem.*, 2006, **45**, 9608; (*c*) R. P. Bontchev and M. Nyman, *Angew. Chem., Int. Ed.*, 2006, **45**, 6670; (*d*) R. Tsunashima, D.-L. Long, H. N. Miras, D. Gabb, C. P. Pradeep and L. Cronin, *Angew. Chem., Int. Ed.*, 2010, **49**, 113.

6 (*a*) M. Nyman, L. J. Criscenti, F. Bonhomme, M. A. Rodriguez and R. T. Cygana, *J. Solid State Chem.*, 2003, **176**, 111; (*b*) C. A. Ohlin, E. M. Villa and J. C. Fettinger, *Dalton Trans.*, 2009, **15**, 2677; (*c*) C. A. Ohlin, E. M. Villa, J. C. Fettinger and W. H. Casey, *Angew. Chem., Int. Ed.*, 2008, **47**, 5634.

7 (*a*) G. Guo, Y. Xu, J. Cao and C. Hu, *Chem. Commun.*, 2011, **47**, 9411; (*b*) G. Guo, Y. Xu, J. Cao and C. Hu, *Chem.–Eur. J.*, 2012, **18**, 3493; (*c*) P. Huang, C. Qin, X.-L. Wang, C.-Y. Sun, G.-S. Yang, K.-Z. Shao, Y.-Q. Jiao, K. Zhou and Z.-M. Su, *Chem. Commun.*, 2012, **48**, 103; (*d*) J.-H. Son, C. A. Ohlin, R. L. Johnson, P. Yu and W. H. Casey, *Chem.–Eur. J.*, 2013, **19**, 5191; (*e*) J.-Q. Shen, Q. Wu, Y. Zhang, Z.-M. Zhang, Y.-G. Li, Y. Lu and E.-B. Wang, *Chem.–Eur. J.*, 2014, **20**, 2840; (*f*) J.-Q. Shen, Y. Zhang, Z.-M. Zhang, Y.-G. Li, Y.-Q. Gao and E.-B. Wang, *Chem. Commun.*, 2014, **50**, 6017; (*g*) P. Huang, E.-L. Zhou, X.-L. Wang, C.-Y. Sun, H.-N. Wang, Y. Xing, K.-Z. Shao and Z.-M. Su, *CrystEngComm*, 2014, **16**, 9582; (*h*) Y.-T. Zhang, C. Qin, X.-L. Wang, P. Huang, B.-Q. Song, K.-Z. Shao and Z.-M. Su, *Inorg. Chem.*, 2015, **54**, 11083.

8 (*a*) J. Niu, P. Ma, H. Niu, J. Li, J. Zhao, Y. Song and J. Wang, *Chem.–Eur. J.*, 2007, **13**, 8739; (*b*) J.-Y. Niu, G. Chen, J.-W. Zhao, P.-T. Ma, S.-Z. Li, J.-P. Wang, M.-X. Li, Y. Bai and B.-S. Ji, *Chem.–Eur. J.*, 2010, **16**, 7082.

9 (*a*) J. Niu, F. Li, J. Zhao, P. Ma, D. Zhang, B. Bassil, U. Kortz and J. Wang, *Chem.–Eur. J.*, 2014, **20**, 9852; (*b*) Z. Liang, D. Zhang, P. Ma, J. Niu and J. Wang, *Chem.–Eur. J.*, 2015, **21**, 8380.

10 (*a*) C. M. Flynn Jr and G. D. Stucky, *Inorg. Chem.*, 1969, **8**, 332; (*b*) J.-H. Son, C. A. Ohlin and W. H. Casey, *Dalton Trans.*, 2013, **42**, 7529; (*c*) Z. Liang, D. Zhang, H. Wang, P. Ma, Z. Yang, J. Niu and J. Wang, *Dalton Trans.*, 2016, **45**, 16173.

11 (*a*) P. Liu, H. Wang, Z. Feng, P. Ying and C. Li, *J. Catal.*, 2008, **256**, 345; (*b*) W. Qi, Y. Wang, W. Li and L. Wu, *Chem.–Eur. J.*, 2010, **16**, 1068; (*c*) A. Wróblewska, E. Ławro and E. Milchert, *Ind. Eng. Chem. Res.*, 2006, **45**, 7365; (*d*) A. Wróblewska, *Appl. Catal., A*, 2006, **309**, 192; (*e*) A. Wróblewska and E. Makuch, *React. Kinet. Catal. Lett.*, 2012, **105**, 451; (*f*) K. Kamata, T. Hirano, S. Kuzuya and N. Mizuno, *J. Am. Chem. Soc.*, 2009, **131**, 6997.

12 (*a*) Z.-M. Zhang, Y.-G. Li, S. Yao, E.-B. Wang, Y.-H. Wang and R. Clérac, *Angew. Chem., Int. Ed.*, 2009, **48**, 1581; (*b*) J. Niu, G. Wang, J. Zhao, Y. Sui, P. Ma and J. Wang, *Cryst. Growth Des.*, 2011, **11**, 1253.

13 J. Fuchs, H. Hartl, W. Schiller and U. Gerlach, *Acta Crystallogr., Sect. B*, 1976, **B32**, 740.

14 I. D. Brown and D. Altermatt, *Acta Crystallogr., Sect. B: Struct. Sci.*, 1985, **41**, 244.

15 P. Ma, G. Chen, G. Wang and J. Wang, *Russ. J. Coord. Chem.*, 2011, **37**, 772.

16 (*a*) M. N. Sokolov, S. A. Adonin, D. A. Mainichev, C. Vicent, N. F. Zakharchuk, A. M. Danilenko and V. P. Fedin, *Chem. Commun.*, 2011, **47**, 7833; (*b*) M. N. Corella-Ochoa, H. N. Miras, A. Kidd, D.-L. Long and L. Cronin, *Chem. Commun.*, 2011, **47**, 8799.

17 (*a*) L. Yang, X. Ma, P. Ma, J. Hua and J. Niu, *Cryst. Growth Des.*, 2013, **13**, 2982; (*b*) W. Huang, D. Wu, P. Zhou, W. Yan, D. Guo, C. Duan and Q. Meng, *Cryst. Growth Des.*, 2009, **9**, 1361.

18 H. Hou, G. Li, L. Li, Y. Zhu, X. Meng and Y. Fan, *Inorg. Chem.*, 2003, **42**, 428.

19 W. Zhao, C. Yang, Z. Cheng and Z. Zhang, *Green Chem.*, 2016, **18**, 995.

20 (*a*) L. Huang, S.-S. Wang, J.-W. Zhao, L. Cheng and G.-Y. Yang, *J. Am. Chem. Soc.*, 2014, **136**, 7637; (*b*) Y. Huo, Z. Huo, P. Ma, J. Wang and J. Niu, *Inorg. Chem.*, 2015, **54**, 406.

21 W. F. Brill, *J. Am. Chem. Soc.*, 1963, **85**, 141.

22 M. Filowitz, R. K. C. Ho, W. G. Klemperer and W. Shum, *Inorg. Chem.*, 1979, **18**, 93.

23 (*a*) G. Sheldrick, *Acta Crystallogr., Sect. A: Found. Crystallogr.*, 1990, **46**, 467; (*b*) G. M. Sheldrick, *Acta Crystallogr., Sect. A: Found. Crystallogr.*, 2008, **64**, 112.